Harmonic Analysis and Pattern Classification of Electrocardiograms for Heart Disease Diagnosis

Alejandro Vidales-Esquivel, Fernando Ornelas-Tellez, *Senior Member, IEEE,* and Jose Ortiz-Bejar, *Member, IEEE*

***Abstract*—Heart disease is a critical issue in improving people's health. Medical research and technology are being developed to obtain accurate diagnoses and treatments. This paper contributes to designing an automated diagnosis system to classify electrocardiogram (ECG) signals to detect cardiac diseases. With respect to other related works, it has the following distinctive characteristics: it is feasible to be implemented in real time, capable of detecting different heart pathologies, and effective in performance. The proposed system is based on Fourier series analysis, employing a dynamical state observer to instantaneously obtain salient features and patterns from the ECG harmonic content, whose information is classified through a K-nearest neighbor algorithm (KNN), named as the classifier, which determines the possible disease. The ECG signals used in this paper are obtained from the freely available PhysioNet databases, containing data to diagnose and classify healthy patients, arrhythmia cases, myocardial infarction, and heart failure. The proposed automated procedure is 93% effective in disease detection for the explored databases, highlighting its potential as a classification tool for ECG-based diagnosis.**

Link to graphical and video abstracts, and to code: https://latamt.ieeer9.org/index.php/transactions/article/view/10091

***Index Terms*—Heart disease diagnosis, Electrocardiogram, Fourier series, Optimal state observer, Harmonic content, Computational classifiers.**

I. Introduction

CURRENTLY, derived from technological developments and electronic devices, different disciplines are improving their information analysis to make better decisions. It is even desirable to automate processes when possible. For instance, mechanisms in medicine are progressing to automate diagnosis, such as identifying cardiac pathologies from biomedical signals through electrocardiogram datasets, among other means. In 2021, around 220,000 people in Mexico died due to cardiovascular diseases, making it the leading cause of death in people over 55 years old [1]. The myocardial infarction was the primary cardiovascular disease and caused 177,000 deaths in 2021 [2]. Meanwhile, 20.5 million deaths were recorded in the same year, according to reports from the World Heart Association [3].

The associate editor coordinating the review of this manuscript and approving it for publication was Roberto S. Murphy (*Corresponding author: Fernando Ornelas-Tellez*).

A. Vidales-Esquivel, Fernando Ornelas-Tellez, and J. Ortiz-Bejar are with the School of Electrical Engineering, Universidad Michoacana de San Nicolas de Hidalgo, F.J. Mugica SN, Morelia, 58030, Mexico (e-mails: alejandro.vidales@umich.mx, fernando.ornelas@umich.mx, and jose.ortiz@umich.mx).

Authors acknowledge the support provided by SECIHTI-Mexico through Project CF-2023-I-1174 within the framework "Ciencia de Frontera 2023".

A. Problem Statement

Electrocardiograms are essential and non-invasive methods for diagnosing heart diseases. However, manual analysis based on human visualization/interpretation of these ECG signals requires highly specialized knowledge, as they can be misinterpreted or misdiagnosed. Currently, an ECG is the result of electrocardiography, as the process of recording the electrical activity of the heart [4]. Previous studies considered for comparison focused on ECG signal classification, regardless of the classification algorithm used. Unlike those approaches, our method combines harmonic estimation through a state observer with an online classification process, offering implementation feasibility. Moreover, this research adopts a multiclass approach, as the classifier can distinguish among four categories corresponding to heart failure, myocardial infarction, arrhythmia, and healthy individuals The ECG signals were obtained from four databases: MIT-BIH Arrhythmia Database for arrhythmia cases [5], BIDMC Congestive Heart Failure Database for heart failure [6], PTB Diagnostic ECG Database for myocardial infarction [7], and MIT-BIH Normal Sinus Rhythm Database for healthy subjects [8]. All databases were integrated into a single dataset to assign labels corresponding to each class. The obtained data can be displayed in an electrocardiograph for medical analysis, and additionally, the data can be digitally stored for computerized analysis purposes. In this sense, the importance of our proposed research is the faster and more automated analysis of ECG signals as a tool for detecting heart pathologies for adequate treatment by a specialist.

B. Gaps in the Literature

Techniques to automatically classify ECG signals and detect heart diseases have been developed. In the case of arrhythmias, for example, authors in [9] use Deep Separable Convolutional Neural Networks with Focal Loss (DSC-FL-CNN) to analyze and classify arrhythmias in ECG signals. In [10], authors use a Mixed-Kernel-based Extreme Learning Machine-based Random Forest binary classifier (MKELM-RF) with 98.1% accuracy in the classification. Also, in [11] employ a deep arrhythmia diagnosis method named Convolutional Neural Network-Bidirectional Long Short-Term Memory (CNN-BLSTM), with an accuracy of 96.59%. In [12], they employ a method to detect arrhythmias based on a combination of a convolutional neural network and short-term memory. Another way to analyze the ECG signals is by preprocessing the information in the frequency domain. For instance, in

[13], the data is preprocessed using the reduced-time Fourier transform, and then image-focused neural networks are applied to classify the ECGs into two categories: healthy or presenting a heart anomaly. However, the method does not give a specific diagnosis of the disease; that is, it only gives the result of whether the patient is healthy or has a heart disease. In this study, little real data is used, and therefore, artificial signals are used to simulate the ECGs. Another alternative is the usage of the Wavelet transform as done in [14], in which a model is developed, and uses a support vector machine (SVM) classifier for the arrhythmias detection. In [15], a K-Nearest Neighbors algorithm is used to classify the ECG signals in the time domain, obtaining an accuracy of 80.9%. Apart from the fact that most studies focus on arrhythmias, there are also investigations dedicated to other diseases, such as in [16], where a system is proposed for detecting myocardial infarction. This model combines a convolutional neural network (CNN) with a long short-term memory model (LSTM), achieving an accuracy of 88.89%. However, in [17], a study is presented on a deep learning system that employs a classification CNN and an LSTM network to extract the spatial and temporal features of ECG signals.

Table I compares the classification system developed in this work with other previously published approaches, all of which were applied to ECG signal analysis. Those published works must, as prerequisites, include classification algorithms for detecting heart diseases from ECG, be computationally efficient for real-time implementation, be useful for different heart pathologies, and contain metrics reports such that our proposal can be evaluated. Most of the reviewed studies focus only on detecting a single pathology and often report a limited set of performance metrics. In contrast, the present study addresses the identification of four different conditions: arrhythmia, heart failure, myocardial infarction, and healthy individuals, which entails a more complex classification task due to the larger number of classes involved. The data set this research has used for studies is the one given in PhysioNet [18].

C. Contributions of the Present Study

This paper contributes by proposing a method for the automated diagnosis of heart diseases. The method uses the Fourier series and an optimal state observer (Kalman filter) to quickly obtain the harmonic content of ECG signals to determine the salient features of different heart pathologies. KNN is used to classify the obtained harmonic content features and identify potential pathologies, keeping our approach simple for future deployment in resource-constrained or online monitoring systems. Nonetheless, other heart disease detection strategy classification algorithms can be used. The accuracy of the proposed diagnosis methodology is greater than 93%.

The organization of the paper is as follows. Section II describes the modeling of the periodic signals using the Fourier series and the design of the optimal observer. Section III presents the optimal estimator as a means of determining the ECG harmonic content quickly, which will be used for classification purposes. Section IV describes the classification method used for heart disease detection and presents the metrics used to evaluate the performance of the proposed system. Finally, Section V presents the conclusions and future work.

II. ECG Modeling through a Fourier Harmonic Description

The heart is an organ that depends on coordinated electrical activity for its proper functioning. The heart muscles carry out this pumping, which can work correctly thanks to electrical impulses [21]. The electrocardiogram is a fundamental tool for recording heart activity and reflects the electrical events during each cardiac cycle [22]. One of the main tasks of the heart is to contract to generate enough pressure in its chambers to properly distribute oxygenated blood throughout the body [23]. Its ability to function as a pump depends on the pumping movements of the atria, ventricles, atrioventricular, and semilunar valves, which direct blood flow within the heart. As mentioned above, heart movements occur over a specific period, known as the cardiac cycle. In more concrete words, the cardiac cycle refers to the events between the start of one heartbeat and the start of the next.

A. The Electrocardiogram

One way to know the health state of the heart is through the ECG, which represents the impulses generated during each cardiac cycle and is graphically recorded and possibly digitally stored. ECG signals are composed of several wave-shaped features that represent the different events of the cardiac cycle, as depicted in Fig. 1, and described as [22], [24]: *P wave:* Represents the depolarization of the atria; *QRS complex:* It is the depolarization of the ventricles, which occurs just before ventricular repolarization; *T wave:* Corresponds to the repolarization of the ventricles, or in other words, the return to a resting state.

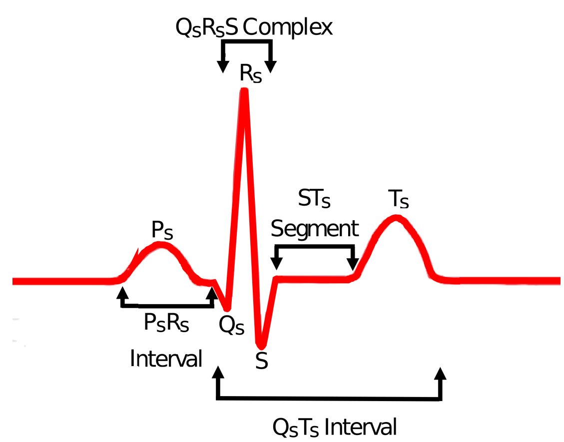

Fig. 1. ECG with their dynamic characteristics.

B. Fourier Harmonic Modeling

The Fourier transform and the Fourier series are widely used tools for analyzing cyclic signals, as exhibited by the ECG.

TABLE I
COMPARISON OF CLASSIFICATION METHODS

Author	Method used	Detected pathologies	Accuracy	Precision	F1 Score	F1 Score (micro)	Recall	AUC
Hao Dang [11]	Deep CNN-BLSTM	Atrial fibrillation	96.54%	N/A	N/A	N/A	99.93%	N/A
Yi Lu [9]	DSC-FL-CNN	Arrhythmia	98.55%	95%	94%	N/A	93%	0.8698 - 0.8965
Chang-Jiang [17]	CNN-LSTM-SE	Heart failure	99.09%	N/A	N/A	N/A	99.03%	N/A
K. Manimekalai [16]	EDN	Myocardial infarction	88.89%	97.76%	93.76%	N/A	86.96%	N/A
Özal Yıldırım [19]	1D-CNN	Arrhythmia	91.33% - 95.2%	89.52% - 92.52%	85.38% - 92.45%	N/A	83.91% - 93.51%	N/A
U. Rajendra [20]	CNN	5 types of arrhythmias	93.47% - 94.03%	N/A	N/A	N/A	96.01% - 96.71%	N/A
This work	KNN	Arrhythmia Heart failure Myocardial infarction Healthy	91.88%	90.74%	92.06%	91.88%	93.10%	0.9336

This proposal employs the latter. Fourier series allows periodic functions/signals to be decomposed into an infinite sum of cosines and sines, which is mathematically described as

$$s(t) = \frac{a_0}{2} + \sum_{n=1}^{N} \left[a_n \cos(w_n\, t) + b_n \sin(w_n\, t)\right] \tag{1}$$

where $s(t)$ is a periodic signal, $\frac{a_0}{2}$ is the constant value (usually named DC component) of the signal, a_n, b_n are the Fourier coefficients, $N \to \infty$ is the number of harmonics (for finite values of N, the series only approximates the signal), the angular frequency $w_n = 2\,n\,\pi\,f$, with $f = \frac{1}{T}$ as the signal frequency of period T. For the purposes of modeling in this paper, it is convenient to present (1) as

$$s(t) = \frac{a_0}{2} + \sum_{n=1}^{N} A_n \sin(w_n\, t + \theta_n) \tag{2}$$

where $A_n = \sqrt{a_n^2 + b_n^2}$ is the amplitude of the sinusoidal function, and $\theta_n = \arctan\left(\frac{b_n}{a_n}\right)$ is the phase angle [25]. Hence, the harmonic content estimation of a signal consists of the determination of a_0, A_n, and θ_n in (2), which can be done through the signal-model-based observer.

C. Periodic Signal Modeling in a State Space

Signal (2) can be modeled in a state space representation, such that a posteriori a state observer can be designed to determine the supposed unknown values of the parameters a_0, A_n and θ_n. To this end, consider the basic case by taking $a_0 = 0$, $N = 1$, the signal amplitude as Am, and employing the following trigonometric identity $\sin(a+b) = \sin(a)\cos(b) + \sin(b)\cos(a)$ for (2), one obtains[1]:

$$s(t) = Am\, \cos\theta\, \sin(w\, t) + Am\, \sin\,\theta \cos(w\, t). \tag{3}$$

[1]The n-subscript is omitted for easy of notation.

By defining the following state space variables as

$$x_1 \triangleq \sin(w\, t); \qquad x_2 \triangleq \cos(w\, t) \qquad \text{and} \qquad y = s(t)$$

the corresponding dynamical description in state space for (3) becomes

$$\begin{aligned} \dot{x}_1 &= w\, x_2 \\ \dot{x}_2 &= -w\, x_1 \\ y &= Am\, \cos\theta\, x_1 + Am \sin\theta\, x_2. \end{aligned} \tag{4}$$

Additionally, for the case when the signal $s(t)$ contains a constant component, given in (2) as $\frac{a_0}{2}$, then the following state variable can be added to (4) as

$$\dot{x}_0 = 0 \tag{5}$$

with initial condition $x(0) = a_0/2$. Then, the complete signal model described by (4)–(5) can be presented in a matrix form as

$$\dot{x} = \begin{bmatrix} 0 & 0 & 0 \\ 0 & 0 & w \\ 0 & -w & 0 \end{bmatrix} x \tag{6}$$

with state vector $x = [x_0\ x_1\ x_2]^T$ and the corresponding output as

$$y = \begin{bmatrix} 1 & Am\cos\theta & Am\sin\theta \end{bmatrix} x. \tag{7}$$

Notice the previous analysis is for one harmonic, i.e., $N = 1$, where the definition of two state variables is needed. Now, the previous modeling procedure can be easily extended to finite values of N, and additionally, from practical considerations, the signal $s(t)$ is assumed to be affected by noise, resulting in a general system as

$$\dot{x} = A\, x + v_1 \tag{8}$$

and output

$$y = C\, x + v_2 \tag{9}$$

where the space state vector $x \in \mathbb{R}^{2N}$ is defined as

$$x = \begin{bmatrix} x_0 & x_1 & x_2 & \cdots & x_{2N-1} & x_{2N} \end{bmatrix}^T$$

and matrices

$$A = \begin{bmatrix} 0 & 0 & 0 & \cdots & 0 & 0 \\ 0 & 0 & w & \cdots & 0 & 0 \\ 0 & -w & 0 & \cdots & 0 & 0 \\ \vdots & \vdots & \vdots & \ddots & \vdots & \vdots \\ 0 & 0 & 0 & \cdots & 0 & w_N \\ 0 & 0 & 0 & \cdots & -w_N & 0 \end{bmatrix}$$

and

$$C = \begin{bmatrix} 1 & A_1\cos\theta_1 & A_1\sin\theta_1 & \cdots & A_N\cos\theta_N & A_N\sin\theta_N \end{bmatrix}$$

while $v_1 \in \mathbb{R}^{2N}$ and $v_2 \in \mathbb{R}$ are the process noise and measurement noise, respectively. Noises v_1 and v_2 are considered Gaussian and zero-mean, with covariance given by $E\left\{v_1(t)\, v_1^T(\tau)\right\} = Q_{v_1}\,\delta(t-\tau)$ and $E\left\{v_2(t)\, v_2^T(\tau)\right\} = R_{v_2}\,\delta(t-\tau)$, respectively, with matrices Q_{v_1} and R_{v_2} nonnegative. Model (8)–(9) will serve for the design of an optimal state estimator (known as Kalman-Bucy filter), as follows.

D. Optimal Observer Design

State observers are algorithms used in dynamical systems to estimate variables (when possible) that are unmeasured or difficult to measure, which is achieved through the available measurements. Hence, considering system (8)–(9), the optimal state observer, based on the Kalman-Bucy filter [26], is designed as

$$\begin{aligned} \dot{\hat{x}} &= A\,\hat{x} + L\,(y - \hat{y}) \\ \hat{y} &= \overline{C}\,\hat{x} \end{aligned} \qquad (10)$$

where the space state $\hat{x} \in \mathbb{R}^{2N}$ is defined as

$$\hat{x} = \begin{bmatrix} \hat{x}_0 & \hat{x}_1 & \hat{x}_2 & \cdots & \hat{x}_{2N-1} & \hat{x}_{2N} \end{bmatrix}^T$$

and $L = P\,\overline{C}^T R_{v_2}^{-1}$ represents the optimal gain of the observer, and P is the solution to the Riccati equation, given as

$$\dot{P} = Q_{v_1} - P\,\overline{C}^T R_{v_2}^{-1}\,\overline{C}\,P + A\,P + P\,A^T. \qquad (11)$$

and

$$\overline{C} = \begin{bmatrix} 1 & k_1 & k_2 & \cdots & k_{2N-1} & k_{2N} \end{bmatrix}^T$$

with $k_1, k_2, \ldots, k_{2N}$ as design parameters. For the observer design, usually the model (8)–(9) is used; nonetheless, notice that the matrix C in (9) is not available since the values for A_n and θ_n are unknown. Hence, it is required to specify a priori the values of the parameters in $\overline{C}$, that is, k_1 to k_{2N}, which a posteriori will be used to calculate the values of the actual matrix C. On its part, matrices Q_{v_1} and R_{v_2} become parameters to be selected such that a desired observer performance can be achieved, and establish a trade-off between state estimation speed and noise immunity. In particular, the values of the matrices are determined by following the procedure described in [27], where a constant value for R_{v_2} is given, and then Q_{v_1} is increased until a satisfactory observer performance is achieved, without affecting the state estimation.

Based on the analysis of (3), the harmonic estimation for Am and θ is given by considering that $\hat{A}m\cos\hat{\theta}\,\sin(w\,t) + \hat{A}m\,\sin\hat{\theta}\cos(w\,t) = k_1\,\hat{x}_1 + k_2\,\hat{x}_2$ and by taking its time derivative, then a set of two algebraic equations and two variables is formed, whose solution becomes

$$\hat{A}m = \sqrt{(k_1^2 + k_2^2)(\hat{x}_1^2 + \hat{x}_2^2)}$$

and

$$\hat{\theta} = -w\,t + \arctan\left(\frac{k_1\,\hat{x}_1 + k_2\,\hat{x}_2}{k_1\,\hat{x}_2 - k_2\,\hat{x}_1}\right).$$

For this research, the parameter of interest is only the amplitude of each n-th harmonic, i.e., A_n. Hence, in a general way, the amplitude estimation of each harmonic in a signal is calculated as

$$\hat{A}_N = \sqrt{\left(k_{2N-1}^2 + k_{2N}^2\right)\left(\hat{x}_{2N-1}^2 + \hat{x}_{2N}^2\right)}. \qquad (12)$$

As an example, numerical values are used in a digital simulation for signal (2), with $N = 1$, $a_0/2 = 0.5$, $A_1 = 0.2$, $w = 0.9$, $\theta_1 = 30\,deg$, $k_1 = 2$, $k_2 = 3$, $Q_{v_1} = diag\{0.01, 0.025, 0.025\}$ and $R_{v_2} = 0.00016$. Then, the estimation of the signal $s(t)$ through $\hat{y}$, and the harmonic content amplitude by means of (12), are depicted in Fig. 2 and Fig. 3, respectively. As can be noted, the variables of the observer converge after a few seconds to the actual values, demonstrating the capability of the harmonic content estimation of the optimal observer over time. Once convergence is achieved, harmonic content can be continuously employed for different purposes, such as frequency-domain analysis and classification.

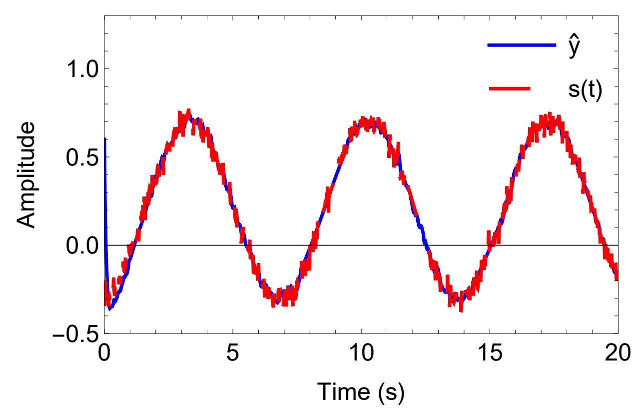

Fig. 2. Estimation of the noisy signal $s(t)$ through the observer output $\hat{y}$, presenting a fast convergence.

Finally, Fig. 4 presents a comparison between the harmonic content of the signal $s(t)$ and the estimated content obtained by the observer. The estimated components are observed to converge toward the real values, exhibiting minimal error, as shown in the Fig. 5. This convergence demonstrates the effectiveness of the state observer in estimating the actual harmonic content.

III. Harmonic Content Determination of ECG

This section presents the optimal observer's usage to estimate the harmonic content of the ECG signals. Based on the

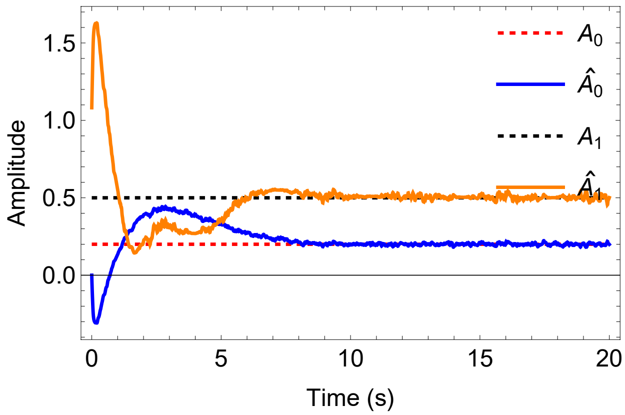

Fig. 3. Time response of the harmonic components estimation toward the actual values contained in $s(t)$.

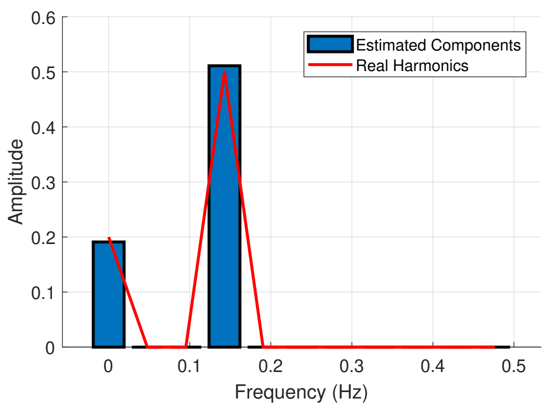

Fig. 4. Comparison between the estimated components and the Fourier spectrum from FFT.

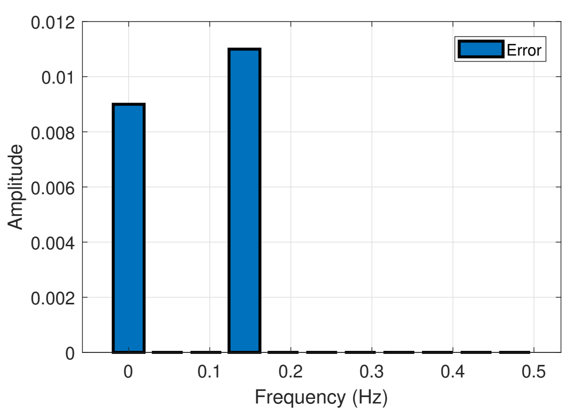

Fig. 5. Error between the estimated harmonics and the obtained fror FFT.

content, its salient characteristics will be used as patterns to classify heart pathologies. Notice that this procedure is performed over time; that is, the harmonic content is determined and, in the same way, immediately classified to obtain the heart diagnosis. Additionally, and only for comparison purposes, the fast Fourier transform (FFT) is used to validate the estimation of the harmonic content. In this sense, while the FFT is used for periodic signals, the proposed estimator can operate under non-periodic conditions, which is a realistic consideration in actual ECG signals.

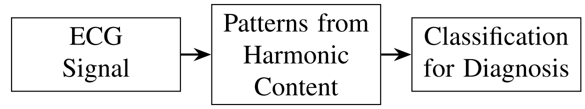

Fig. 6. Process block diagram for the diagnosis composed of three main stages.

A. *Diagnosis General Scheme*

Fig. 6 shows the general scheme of the process, starting with the acquisition of the ECG signal, which is preprocessed by detecting the R peaks to segment each cardiac cycle and normalizing the signals to millivolts (mV) to ensure consistency among records. The optimal observer then uses the preprocessed data to compute the harmonic content, which is classified by a KNN algorithm to perform the diagnosis continuously; that is, once the proposed methodology receives the ECG signal over time from a patient, the classification algorithm immediately provides the possible cardiac pathology.

B. *Simulation Results*

Fig. 7 displays the average spectrum of harmonic amplitudes corresponding to healthy subjects, and those with arrhythmia, heart failure, and myocardial infarction. Each bar represents the average amplitude value for each harmonic component across multiple cycles, highlighting distinctive patterns among conditions that can be used for classification. For the observer simulation, matrix Q_{v_1} is a diagonal matrix with values equal to 10, the scalar matrix $R_{v_2} = 0.01$, and the constant parameter values are $k_{2N-1} = 0.5$ and $k_{2N} = 0.01$.

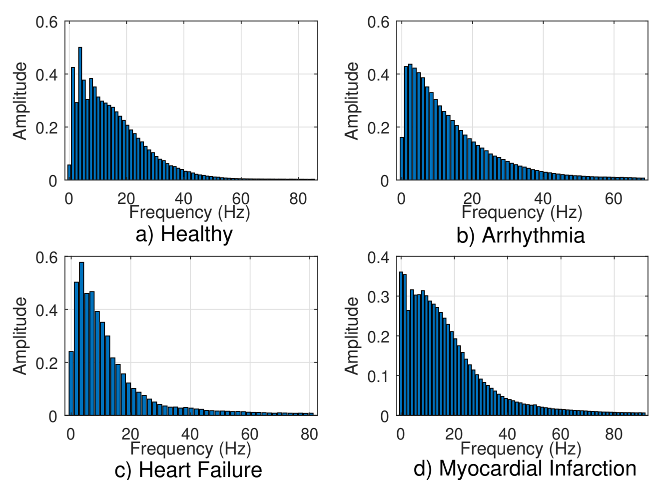

Fig. 7. Average harmonic content (features) of each heart condition to be used for classification purposes: a) Harmonic content of Healthy; b) Harmonic content of Arrhythmia; c) Harmonic content of Heart Failure; d) Harmonic content of Myocardial Infarction.

Fig. 8 displays the estimated harmonic content (blue bars), which is compared with that obtained from Matlab/FFT (red line), showing that the harmonic estimation is equal. Fig. 9

presents the estimation error, which is small, giving confidence in the proposed fast procedure to be used by the classifier. On the other hand, Fig. 10 shows the convergence over time of the optimal state observer toward the references provided by the Matlab/FFT. The figure is divided into four panels: the first shows the DC component A_0, followed by the first, second, and third harmonics, denoted as A_1, A_2, and A_3, respectively. In each panel, the blue line represents the estimated component, while the red dashed line corresponds to the FFT reference. It can be observed that the estimation converges to the reference values at approximately 4 seconds. Finally, the classifier processes the harmonic content, as described below.

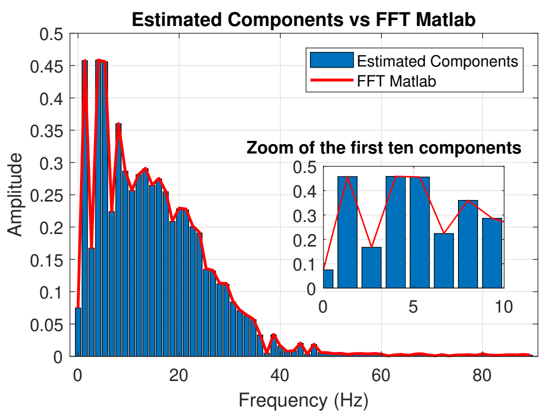

Fig. 8. Harmonic comparison to validate the proposed observer estimation: FFT Matlab vs estimated.

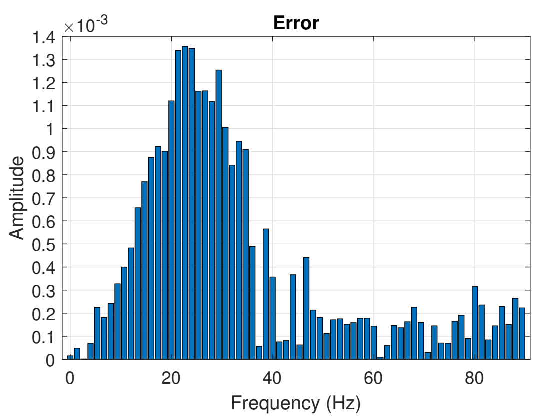

Fig. 9. Error between the harmonics calculated through the FFT and their estimation by the proposed observer.

IV. ECG Classification and Diseases Detection

ECG classification is necessary to determine different heart diseases. The number of classes to classify depends on the number of available classes in the training dataset. In this research, including the healthy condition, three cardiac pathologies are also considered: arrhythmia, heart failure, and myocardial infarction. The pathology classification will be performed by identifying patterns in the harmonic content of the ECG by using a machine learning algorithm. The patient databases are obtained from the PhysioNet website

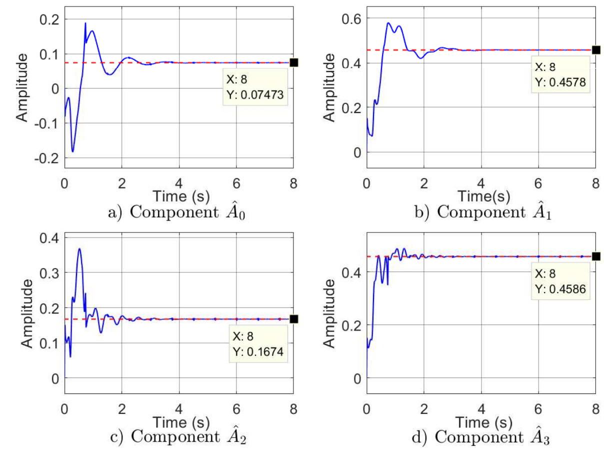

Fig. 10. Harmonics along time that the observer continuously estimates: a) Time evolution of $\hat{A}_0$; b) Time evolution of $\hat{A}_1$; c) Time evolution of $\hat{A}_2$; d) Time evolution of $\hat{A}_3$.

[18]. TABLE II presents the number of patients used for each pathology and their distribution between the training and validation sets, which together constitute the database used in this study. Each signal contains 10 cardiac cycles, resulting in a total of 1050 cardiac cycles analyzed and used to train the KNN classifier.

TABLE II
Database for the Classifier Training and Validation

Pathology	**Patients**	**Training Heartbeats**	**Validation Heartbeats**
Heart Failure	10	70	30
Myocardial Infarction	42	290	130
Arrhythmia	29	200	90
Healthy	24	170	70
Total patients	**105**	**730 cycles**	**320 cycles**

The Phystionet ECG signal was employed to evaluate the performance of the proposed system. Our experiments consist of two steps. First, a profiling step through a cross-validation. The 70% of the total data is used to create a 70-30 training-validation partition. A 5-fold cross-validation is used to assess the classifier's consistency and generalization capabilities. In a second step, the remaining 30% of the dataset is separated as a testing set. It is worth mentioning that training and testing are generated from records of different patients (i.e., no heartbeats from the same patient appear in both sets) to reduce data leakage and bias when evaluating the classifier performance over new data. There are various techniques for ECG classification, such as Traditional ECG interpretation by experts, where doctors visually analyze an ECG to diagnose heart problems, mainly when visible issues can be identified in the ECG, such as changes in the duration of the P_s and T_s waves or changes in the amplitude of the QRS complex. Another ECG classification method is the classification by Machine Learning.

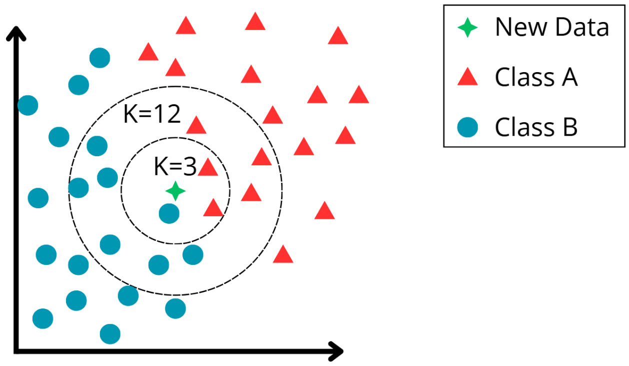

Fig. 11. K-Nearest Neighbor scheme to classify new data from the classifier parameter configuration.

A. K-Nearest Neighbors

The KNN algorithm is chosen due to its simplicity and non-parametric nature. The latter allows KNN to adapt to complex decision boundaries by considering local data distributions rather than relying on global ones. This characteristic enables minority-class instances to influence classification decisions more effectively without requiring assumptions about the underlying distribution, which makes KNN especially useful for balanced and imbalanced datasets [28] This research uses the KNN algorithm to classify ECG signals according to their harmonic characteristics. Although KNN has been applied in other studies, it is implemented differently in this work since multiple classes are used. KNN is a supervised machine learning classifier, meaning that it is trained using a labeled dataset [29]. In our case, the database did not originally contain labeled classes, so the data are manually labeled to make it suitable for a classification task. The algorithm follows the following steps to classify a new data point whose class is unknown: *(a)* distance computation: the distance between the new data point and all training data points is reckoned using a distance function. In MATLAB, Euclidean, Chebychev, Correlation, Cosine, and Mahalanobis are available. Generally, Euclidean distance is used, as done in this research; *(b)* identify the nearest neighbors: the K closest data points to the new data point are selected; *(c)* classify: the class of new data is computed as a majority vote decision, selecting the most common class (i.e., the mode) between the K nearest neighbors.

Fig. 11 illustrates the classification process, in which the KNN algorithm is observed using a new data point and $K = 3$; then, in this case, the 3 closest data points are considered, and the majority vote results in class A because there are 2 data of class A and 1 data of class B. Now, for $K = 12$, the majority vote considers class B the winner because there are 7 data from class B and 5 from class A, and the new data will be classified as class B. An alternative to classifying is by a weighted vote using the distance between the data query and its neighbors. In this case, the closest points will have greater weight in the decision, while the farthest ones have less influence.

B. Metrics

For comparison purposes, in addition to KNN, two widely used classification systems, Support Vector Machine (SVM) and Multi Layer Perceptron (MLP), are used over the generated features, and the results for the metrics used to evaluate the classifier performance and their values are shown in Table III. The *Accuracy* expresses how well the classifier works in terms of the ratio of correct predictions to the total number of predictions [30]. The *Precision* measures how many of the predicted classes for a specific class are correct. [30]. *Recall* calculates the number of actual instances of a specific class that were correctly predicted [30]. The *F1 score* is a metric that combines precision and recall in a single value. This metric is particularly useful when working with datasets with imbalanced classes [31]. The area under the curve (*AUC*) is a metric used to evaluate the performance of a classification model, specifically regarding its ability to discriminate between classes. The AUC varies between 0.5 and 1, where a value closer to 1 means a better classifier, a value of 1 is a perfect classifier, and a value closer to 0.5 is equivalent to a very bad classifier; this means that the classifier is working randomly. The AUC score of a classifier represents the probability that the classifier ranks a randomly chosen positive instance higher than a randomly chosen negative instance [32]. In a multiclass context, a high AUC score suggests that the classifier effectively ranks instances of each class higher than those of other classes, indicating strong discriminatory ability. In this research, the classifiers were implemented in MATLAB. The KNN was configured with two closest neighbors ($K = 2$). The MLP was trained with three hidden layers, each with 30 neurons and a Levenberg-Marquardt optimization algorithm. The SVM model uses a polynomial kernel of order 3, an approach one-vs-all for multiclass classification.

TABLE III
PERFORMANCE METRICS FOR EACH CLASSIFIER

Metric	**KNN**	**MLP**	**SVM**	**95% CI (KNN)**
Accuracy	91.88%	74.39%	64.93%	90.19–93.57%
Precision	90.74%	71.95%	62.70%	88.75–92.73%
Recall	93.10%	74.01%	63.83%	91.54–94.66%
F1 Score	92.06%	73.22%	56.25%	91.19–92.93%
F1 Score (Micro)	91.88%	74.39%	64.93%	90.19–93.57%
AUC	93.36%	90.62%	86.95%	91.48–95.24%

Finally, Fig. 12 shows the average confusion matrix; the values are normalized per class. The diagonal values are close to 1.00, indicating that most samples are correctly classified. The exceptions appear between the Heart Failure and Arrhythmia classes (up to 4%) and between Myocardial Infarction and Arrhythmia (1%), suggesting that these categories share partially similar ECG features in the generated features.

C. Confidence

Confidence in classification models evaluates how certain the model is about its predictions. In this research, the receiver operating characteristic (ROC) curve will be used to evaluate the performance of the KNN classifier. The ROC curve is a visual representation of the model performance, which is

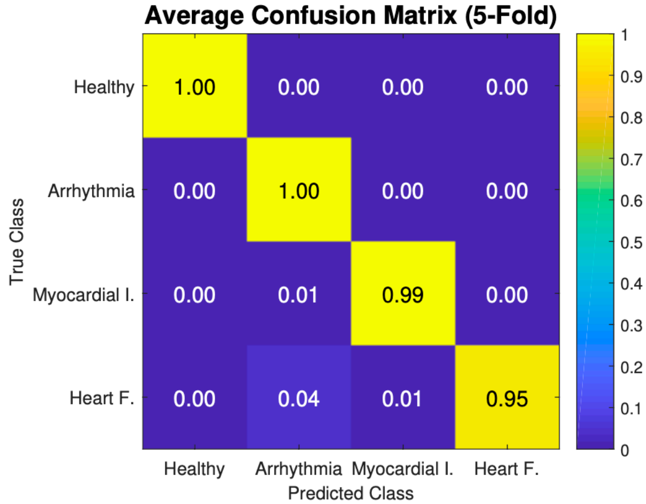

Fig. 12. Average confusion matrix obtained across 5-fold cross-validation, showing the mean normalized classification performance per class.

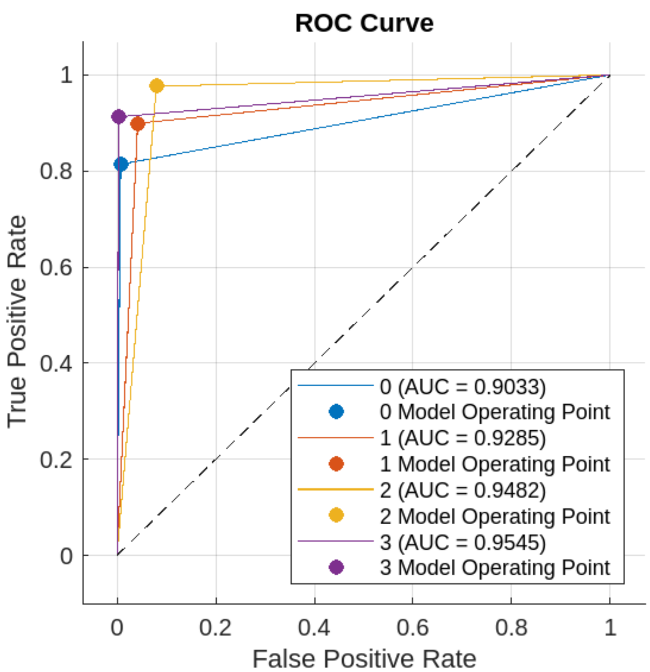

Fig. 13. Curve ROC to evaluate the performance of the classifier.

the relationship between the false positive rate and the true positive rate [33]. The false positive rate is the data that is false but classified as true, and the true positive rate is the true data that is classified as true [32]. For the KNN classifier, the ROC curves shown in Fig. 13 are generated including four classes: Class 0 (Healthy person), class 1 (Arrhythmia), class 2 (Myocardial Infarction) and class 3 (Heart failure). These curves are interpreted by the AUC, whose results are presented in Table III.

D. Results Discussion

As part of this research, work is progressing in evaluating the real-time implementation of the proposed diagnosis methodology by using current technology, as Arduino, micro-computers, among others. It is worth mentioning that the proposed strategy could be used in analyzing general cyclic signals, as they appear in biomedical systems or other electrical signals, where it is required to determine frequency-domain features in real-time, such as the harmonic content, tuning of active filters, etc. One of the limitations of the proposed methodology is the required computational effort when a signal contains a high harmonic content, since the observer will become of high dimension, and as a consequence, the classifier processing will be demanding as well; nonetheless, if the process to be analyzed has slow dynamics, a current processor unit could solve the needed computations. For the proposed heart diagnosis system, it is expected to obtain an economical and accessible technological solution to perform the required algorithms. Although the system works correctly with the available data, an effort is being made to have a larger database to improve the results; hence, these limitations do not affect the performance of the current diagnosis system, which presents a high performance that can be seen in the metrics presented in TABLE III. From the results, KNN outperforms SVM and MLP in all evaluated metrics. Additionally, the KNN results for all metrics, along with the narrow 95% confidence intervals (CI), indicate a stable and consistent performance across the cross-validation folds [34]. Despite no explicitly applied resampling techniques or class weighting adjustments, the combination of high F1, micro F1, and AUC scores indicates that the proposal exhibits robust generalization capabilities and does not favor majority classes. Using the F1 score allows every class to contribute equally to the overall system performance, regardless of frequency. At the same time, F1 micro evaluates the model considering the imbalance in sample distribution, and the achieved AUC score suggests that the model exhibits strong discrimination between classes (including minority class heart failure).

From Fig. 13 it can be seen that the classifier used in this research has a better performance for class 3 (Heart failure) with a 95.45% probability of being correct for that pathology and the lowest but not bad performance for class 0 (Healthy person) with 90.33%. Finally, the system was tested for the four categories: heart failure, myocardial infarction, arrhythmia, and healthy people, using new ECG test signals that were not included in the training of the classifier. Each ECG consisted of 10 cardiac cycles, and predictions were made cycle by cycle to finally assign a final pathology to each patient based on the category with the highest number of predictions. The effectiveness of the research proposal is summarized as follows. The results presented in Table IV show a performance greater than 93%, highlighting the effectiveness in correctly classifying ECG signals in the four categories: heart failure, myocardial infarction, arrhythmia, and healthy individuals. The metrics obtained emphasize the ability of the system to provide accurate and reliable classifications.

V. Conclusions and Future Work

At this research stage, the paper results show high confidence levels and effectiveness in classifying three pathologies:

TABLE IV
VALIDATION RESULTS OF THE HEART DISEASE DETECTION

Condition	Patients	Analyzed Heartbeats	Effectiveness
Heart Failure	3	30	93.3%
Myocardial Infarction	13	130	93.7%
Arrhythmia	9	90	93.6%
Healthy	7	70	93.1%

arrhythmia, myocardial infarction, and heart failure, as well as the condition of a healthy person. This contribution demonstrated its efficacy and is a functional method for automatically detecting cardiac pathologies. However, the proposed methodology needs to be tested in real medical scenarios to evaluate its desired effectiveness. As part of future research, work is progressing to improve the classification algorithm to increase its effectiveness. A medical procedure involving a heart specialist doctor is also being outlined to include new data on the different pathologies to evaluate the automated diagnosis system. Currently, the design of an experimental prototype to perform tests on real patients is in progress, where the real-time implementation can also be evaluated.

REFERENCES

[1] Secretaría de Salud, “Hasta 80% de decesos por enfermedades cardiovasculares son prevenibles: Hospital general de méxico.” [Online]. Available: https://www.gob.mx/salud/prensa/319-hasta-80-de-decesos-por-enfermedades-cardiovasculares-son-prevenibles-hospital-general-de-mexico

[2] Secretaría de Salud , “Cada año, 220 mil personas fallecen debido a enfermedades del corazón.” [Online]. Available: https://www.gob.mx/salud/prensa/490-cada-ano-220-mil-personas-fallecen-debido-a-enfermedades-del-corazon

[3] World Heart Federation, “World heart report 2023: Confronting the world’s number one killer,” Geneva, Switzerland, 2023. [Online]. Available: https://world-heart-federation.org/wp-content/uploads/World-Heart-Report-2023.pdf

[4] W. Uribe, M. Duque, and E. Medina Arango, “Electrocardiografía y arritmias,” *Revista Iberoamericana de Arritmología*, pp. 1–145, 2010, dOI: 10.5031/v1i2.RIA1012.

[5] G. Moody and R. Mark, “MIT-BIH Arrhythmia Database,” https://doi.org/10.13026/C2F305, 2001, available on PhysioNet.

[6] D. S. Baim, W. S. Colucci, E. S. Monrad, H. S. Smith, R. F. Wright, A. A. Lanoue, D. F. Gauthier, B. J. Ransil, W. Grossman, and E. Braunwald, “Bidmc congestive heart failure database,” https://doi.org/10.13026/C29G60, 1986, available on PhysioNet. Subset of data described in J. American College of Cardiology, vol. 7, no. 3, pp. 661–670, Mar. 1986.

[7] R. Bousseljot, D. Kreiseler, and A. Schnabel, “PTB Diagnostic ECG Database,” https://doi.org/10.13026/C28C71, 1995, available on PhysioNet.

[8] T. S. Lugovaya, “ECG-ID Database,” https://doi.org/10.13026/C2J01F, 2005, available on PhysioNet.

[9] Y. Lu, M. Jiang, L. Wei, J. Zhang, Z. Wang, B. Wei, and L. Xia, “Automated arrhythmia classification using depthwise separable convolutional neural network with focal loss,” *Biomedical Signal Processing and Control*, vol. 69, p. 102843, 2021, https://doi.org/10.1016/j.bspc.2021.102843.

[10] P. Yang, D. Wang, W.-B. Zhao, L.-H. Fu, J.-L. Du, and H. Su, “Ensemble of kernel extreme learning machine based random forest classifiers for automatic heartbeat classification,” *Biomedical Signal Processing and Control*, vol. 63, p. 102138, 2021, https://doi.org/10.1016/j.bspc.2020.102138.

[11] H. Dang, M. Sun, G. Zhang, X. Qi, X. Zhou, and Q. Chang, “A novel deep arrhythmia-diagnosis network for atrial fibrillation classification using electrocardiogram signals,” *IEEE Access*, vol. 7, pp. 75 577–75 590, 2019, dOI: 10.1109/ACCESS.2019.2918792.

[12] S. L. Oh, E. Y. Ng, R. S. Tan, and U. R. Acharya, “Automated diagnosis of arrhythmia using combination of cnn and lstm techniques with variable length heart beats,” *Computers in Biology and Medicine*, vol. 102, 06 2018, https://doi.org/10.1016/j.compbiomed.2018.06.002.

[13] J. Quer Martínez, “Analisis de electrocardiogramas mediante tecnicas de ingenieria para la deteccion de enfermedades cardiacas,” Master’s thesis, Universidad Pontificia De Comillas, 2019. [Online]. Available: http://hdl.handle.net/11531/31001

[14] S. Kumar Saini and R. Gupta, “Artificial intelligence methods for analysis of electrocardiogram signals for cardiac abnormalities: state-of-the-art and future challenges,” *Springer/Artificial Intelligence Review*, vol. 55, pp. 1519–1565, 2021, https://doi.org/10.1007/s10462-021-09999-7.

[15] D. Losada, J. Gómez, and J. Vela, “Classification of ECG signals using machine learning techniques,” *Academic Journal of Interdisciplinary Studies*, vol. 13, no. 3, pp. 1–12, 2024, https://doi.org/10.36941/ajis-2024-0067.

[16] K. Manimekalai and D. Kavitha, “Deep learning methods in classification of myocardial infarction by employing ECG signals,” *Indian Journal of Science and Technology*, vol. 13, no. 28, pp. 2823–2832, 2020, https://doi.org/10.17485/IJST/v13i28.445.

[17] C.-J. Zhang, Yuan-Lu, F.-Q. Tang, H.-P. Cai, Y.-F. Qian, and Chao-Wang, “Heart failure classification using deep learning to extract spatiotemporal features from ECG,” *BMC Medical Informatics and Decision Making*, vol. 24, no. 17, pp. 1–17, 2024, https://doi.org/10.1186/s12911-024-02415-4.

[18] “Physionet.” [Online]. Available: https://physionet.org/

[19] O. Yıldırım, P. Pławiak, R.-S. Tan, and U. R. Acharya, “Arrhythmia detection using deep convolutional neural network with long duration ECG signals,” *Computers in Biology and Medicine*, vol. 102, pp. 411–420, 2018, https://doi.org/10.1016/j.compbiomed.2018.09.009.

[20] U. R. Acharya, S. L. Oh, Y. Hagiwara, J. H. Tan, M. Adam, A. Gertych, and R. S. Tan, “A deep convolutional neural network model to classify heartbeats,” *Computers in Biology and Medicine*, vol. 89, pp. 389–396, 2017, https://doi.org/10.1016/j.compbiomed.2017.08.022.

[21] T. Newman and article reviewed by Dr. Payal Kohli M.D. FACC, “El corazón: Anatomía, cómo funciona y más,” 2021. [Online]. Available: https://www.medicalnewstoday.com/articles/es/el-corazon

[22] J. E. Hall, *Guyton and Hall: Textbook of Medical Physiology*. Philadelphia, PA, USA: Saunders/Elsevier, 2011, https://doi.org/10.4103/sni.sni_327_17.

[23] J. Tamargo and E. Delpón, *La función de bomba del corazón*. New York, NY: McGraw-Hill Education, 2016. [Online]. Available: accessmedicina.mhmedical.com/content.aspx?aid=1132161556

[24] S. N. M. S. Ismail, N. A. A. Aziz, S. Z. Ibrahim, S. W. Nawawi, S. Alelyani, M. Mohana, and L. C. Chun, “Evaluation of electrocardiogram: numerical vs. image data for emotion recognition system,” *F1000Research*, vol. 10, no. 1114, p. 1114, 2021, https://doi.org/10.12688/f1000research.73255.2.

[25] S. Ramos-Paz, F. Ornelas-Tellez, and J. J. Rico-Melgoza, “Dynamic harmonics–interharmonics identification and compensation through optimal control of a power conditioning application,” *Electrical Engineering*, vol. 104, pp. 3589–3602, 2022, https://doi.org/10.1007/s00202-022-01570-z.

[26] B. D. O. Anderson and J. B. Moore, *Optimal Control: Linear Quadratic Methods*. Englewood Cliffs, NJ, USA: Prentice-Hall, 1990, https://dl.acm.org/doi/book/10.5555/79089.

[27] H. Kwakernaak and R. Sivan, *Linear Optimal Control Systems*. New York, NY, USA: Wiley-Interscience, 1972. [Online]. Available: https://dl.acm.org/doi/10.5555/578807

[28] R. K. Halder and S. Saha, “Enhancing k-nearest neighbor algorithm: A comprehensive review and performance analysis of modifications,” *Journal of Big Data*, vol. 11, no. 1, pp. 1–29, 2024, 10.1186/s40537-024-00973-y.

[29] S. Uddin, M. A. M. Ibtisham Haque, Haohui Lu, and E. Gide, “Comparative performance analysis of K-nearest neighbour (KNN) algorithm and its different variants for disease prediction,” *Scientific Reports*, vol. 12, no. 6256, pp. 1–11, 2022, https://doi.org/10.1038/s41598-022-10358-x.

[30] M. Sokolova, N. Japkowicz, and S. Szpakowicz, “Beyond accuracy, F-score and ROC: A family of discriminant measures for performance evaluation,” in *AI 2006: Advances in Artificial Intelligence, Lecture Notes in Computer Science*, vol. Vol. 4304, 01 2006, pp. 1015–1021, https://dl.acm.org/doi/10.1007/11941439_114.

[31] J. Han, M. Kamber, and J. Pei, *Data mining concepts and techniques*, 3rd ed. Waltham, Mass.: Morgan Kaufmann Publishers, 2012, https://dl.acm.org/doi/10.5555/1972541.

[32] T. Fawcett, “Introduction to ROC analysis,” *Pattern Recognition Letters*, vol. 27, pp. 861–874, 2006, https://doi.org/10.1016/j.patrec.2005.10.010.

[33] S. Gajjalavari and V. Vardhan, "Multi-class classification using mixtures of univariate and multivariate ROC curves," *Journal of Biostatistics and Epidemiology*, vol. 8, no. 2, pp. 208–233, 2022, https://doi.org/10.18502/jbe.v8i2.10418.

[34] T. Hastie, R. Tibshirani, and J. Friedman, *The Elements of Statistical Learning: Data Mining, Inference, and Prediction*, 2nd ed. New York: Springer, 2009, chapter 7: Model Assessment and Selection. [Online]. Available: https://web.stanford.edu/~hastie/ElemStatLearn/

Alejandro Vidales Esquivel received the B.Sc. degree in electronic engineering from the Universidad Michoacana de San Nicolas de Hidalgo (UMSNH), Morelia, Mexico, in 2021. Currently, he is completing an M.Sc. degree in electrical engineering at the UMSNH. His research focuses on harmonic analysis of ECG signals, development of state observers for system estimation, biomedical signal modeling, and the application of machine learning techniques for computer-based medical diagnosis.

Fernando Ornelas-Tellez (M'11, SM'21) received the B.Sc. degree from the Instituto Tecnologico de Morelia (ITM), Morelia, Mexico, in 2005 and the M.Sc. and D.Sc. degrees in electrical engineering from the Advanced Studies and Research Center, National Polytechnic Institute (CINVESTAV-IPN), Guadalajara, Mexico, in 2008 and 2011, respectively. Since 2012, he has been with the Universidad Michoacana de San Nicolas de Hidalgo, where he is currently a professor of Electrical Engineering graduate programs. His research interest centers on optimal control, neural control, sliding modes control, and passivity, and their applications to smart grids, power electronics, mechanical systems, and electrical machines.

Jose Ortiz-Bejar (M'14) received the Ph.D. degree in data science from INFOTEC, Unidad Aguascalientes, in 2020. He is currently an associate professor with the Michoacan University of San Nicolás de Hidalgo. He has served as an Organizer of ROPEC and IEEE T&DLA conferences. His research interest centers on machine learning applied to power systems analysis, text categorization, and clustering.